Pharm Res (2014) 31:946–958
DOI 10.1007/s11095-013-1214-1

RESEARCH PAPER

Solidified Self-Nanoemulsifying Formulation for Oral Delivery of Combinatorial Therapeutic Regimen: Part II *In vivo* Pharmacokinetics, Antitumor Efficacy and Hepatotoxicity

Amit K. Jain • Kaushik Thanki • Sanyog Jain

Received: 4 July 2013 / Accepted: 18 September 2013 / Published online: 18 October 2013

ABSTRACT

Purpose The present work focuses on the *in vivo* evaluation of tamoxifen and quercetin combination loaded into solid self-nanoemulsifying drug delivery system (s-Tmx-QT-SNEDDS).

Methods Lyophilization was employed to prepare s-Tmx-QT-SNEDDS using Aerosil 200 as carrier. The developed formulation was evaluated for *in vitro* cell cytotoxicity, *in vivo* pharmacokinetics, antitumor efficacy and toxicity studies.

Results *In vivo* pharmacokinetics revealed ~8-fold and ~4-fold increase in oral bioavailability of tamoxifen and quercetin, respectively as compared to free counterparts. s-Tmx-QT-SNEDDS exhibited significantly higher cell cytotoxicity, as compared to free drug combination revealing ~32-fold and ~22-fold higher dose reduction index for tamoxifen and quercetin, respectively estimated using median effect dose analysis. s-Tmx-QT-SNEDDS could suppress tumor growth in DMBA induced tumor bearing animals by ~80% in contrast to ~35% observed with tamoxifen citrate. The significant appreciation in antitumor efficacy was further supported by normalized levels of tumor angiogenesis markers (MMP-2 and MMP-9). Finally, complete obliteration in tamoxifen induced hepatotoxicity was observed upon administration of developed formulation in contrast to that of clinically available tamoxifen citrate when measured as function of hepatotoxicity markers and histopathological changes.

Conclusions In nutshell, co-encapsulation of quercetin with tamoxifen in solid SNEDDS poses great potential in improving the therapeutic efficacy and safety of tamoxifen.

KEY WORDS DMBA induced breast tumor · hepatotoxicity · quercetin · SNEDDS · tamoxifen

INTRODUCTION

Co-administration of an antioxidant, having anti-proliferative and antioxidant properties, could be of great interest for augmenting overall antitumor efficacy and reducing the toxicity of anticancer drugs (1,2). Tamoxifen (Tmx), a non-steroidal anti-estrogen, is a widely used hormonal drug for prevention and treatment of estrogen positive breast cancer at multiple stages (3). However, extensive hepatic first pass metabolism limits its oral bioavailability and aggravate the multiple symptoms of hepatotoxicity (4–7). In this regard, quercetin (QT), a pentaflavanol, acts as potential free radical scavenger (8,9) as well as an anti-proliferative agent (10–13). QT, being a free radical scavenger enhances antioxidant enzyme activity, inhibit mitochondrial lipid and protein oxidation by scavenging the reactive oxygen species (ROS) (14). A number of reports have been published revealing the propensity of QT to combat the liver damage against drug or chemically induced toxic free radicals (15–18). However, until now effect of QT on Tmx induced hepatotoxicity has not been explored. Additionally, QT also possesses anticancer property by virtue of its multiple molecular mechanisms in cancer cells (19). Over the last decade, co-administration of QT with Tmx has been explored for improving anticancer efficacy as well as preventing the tumor angiogenesis (20,21). Of note, both the drugs binds with estrogen receptors, but at the dissimilar site that can rationalize the synergistic cytotoxicity of the said combination

Electronic supplementary material The online version of this article (doi:10.1007/s11095-013-1214-1) contains supplementary material, which is available to authorized users.

A. K. Jain · K. Thanki · S. Jain (✉)
Centre for Pharmaceutical Nanotechnology
Department of Pharmaceutics
National Institute of Pharmaceutical Education and Research (NIPER)
Sector 67, S.A.S. Nagar, Mohali, Punjab 160062, India
e-mail: sanyogjain@niper.ac.in
e-mail: sanyogjain@rediffmail.com

(22). However, poor oral bioavailability of QT (rats ~17%; human ~2%) owing to poor aqueous solubility, pre-systemic metabolism and first pass hepatic metabolism limits its oral deliverability and utility in combination with Tmx (23,24). Furthermore, undesired pharmacokinetics and pharmacodynamics interactions may arise subsequent to oral administration of free Tmx and QT (2). Hence, an alternate delivery system consisting of said combination in the therapeutic dose is desirable to achieve the substantial therapeutic benefit from Tmx-QT combination. A variety of novel technologies such as liposomes (25,26), polymeric nanoparticles (27–30), polymer drug conjugates (31,32), mesoporous silica nanoparticles (33) and dendrimers (34), have been investigated for the co-encapsulation of various therapeutic relevant combinations. However, the efficient use of these systems is limited due to their complex manufacturing steps, high production cost and poor drug loading capacity, especially of antioxidants.

Over the last few decades, solid self-nanoemulsifying drug delivery system (s-SNEDDS) represents one of the most popular, commercially meaningful and readily scalable delivery vehicles for improving the oral bioavailability of poorly aqueous soluble or highly lipophilic drugs (35,36). s-SNEDDS offers the combined advantages of conventional lipid based drug delivery system (i.e. enhanced solubility and bioavailability) with those of solid dosage forms (e.g. low production cost, convenience of process control, high stability and reproducibility, better patient compliance) (37). Carrying forward with the Part I of the present work, which specifically deals with formulation development, optimization and solidification of SNEDDS, the Part II demonstrates the efficacy potential and *in vivo* performance of the developed formulation, assessed as a function of *in vivo* pharmacokinetics and *in vivo* anticancer efficacy in DMBA-induced breast tumor model. In course of extensive *in vitro* studies, we have established the intracellular localization and cytotoxicity of s-Tmx-QT-SNEDDS in MCF-7 cell lines. Following the completion of tumor inhibition studies, we revealed that s-Tmx-QT-SNEDDS lead to marked reduction in the levels of tumor angiogenesis as well as hepatotoxicity markers as compared to commercially available Tmx citrate salt as well as its combination with free QT.

MATERIALS AND METHODS

7,12-dimethylbenz [α] anthracene (DMBA), 2,2-Diphenyl-1-picrylhydrazyl (DPPH), trypsin-EDTA, (3-(4,5-Dimethyl-2-thiazolyl)-2,5-diphenyl-2H-tetrazolium bromide) (MTT), coumarin-6 (C-6), triton X-100, 4′,6-diamidino-2-phenylindole (DAPI) were purchased from Sigma, USA. Dulbecco's modified Eagle's medium (DMEM), fetal bovine serum (FBS), antibiotics (Antibiotic-antimycotic solution) and Hanks's balanced salt solution (HBSS) were purchased from PAA Laboratories GmbH, Austria. Dimethyl sulphoxide (DMSO, AR grade), ethyl acetate (LR grade), acetonitrile (HPLC grade), methanol (HPLC grade) were purchased from Fischer Scientific, USA. Ultra-pure deionized water (SG water purification system, Barsbuttel, Germany) was used for all the experiments. All other reagents used were of analytical grade.

Preparation of Liquid Tmx-QT-SNEDDS

Liquid Tmx-QT-SNEDDS was prepared by using Capmul MCM EP, Cremophor RH 40 and Labrafil 1944 CS as oil, surfactant and co-surfactant, respectively. Briefly, excess amount of Tmx and QT were added to glass vial containing the mixture of Capmul MCM EP (400 mg), Cremophor RH 40 (300 mg) and Labrafil 1944 CS (300 mg), followed by vortexing for 2 min to obtain a homogenous mixture. The resultant mixture was allowed to incubate in shaker water bath (Lab Tech, Korea) operated at 50 strokes/min for 72 h at 37°C to attain the equilibrium. The mixture was centrifuged at 5,000 rpm for 5 min to separate insoluble drugs followed by heating of supernatant at 40–45°C to form an isotropic liquid Tmx-QT-SNEDDS.

Preparation of Solid Tmx-QT-SNEDDS (s-Tmx-QT-SNEDDS)

s-Tmx-QT-SNEDDS was prepared by step-wise lyophilization of liquid Tmx-QT-SNEDDS in the presence of Aerosil 200 (38). Briefly, liquid Tmx-QT-SNEDDS (200 mg) was thoroughly mixed with deionized water (5 ml) and equilibrated for 10 min to form a nanoemulsion, which was then mixed with 200 mg of Aerosil 200 and finally lyophilized using the step-wise freeze-drying cycle.

Characterization of s-Tmx-QT-SNEDDS

Transmission Electron Microscopy (TEM) Upon Reconstitution

The morphology of nanoemulsion obtained upon reconstitution of s-Tmx-QT-SNEDDS was evaluated by transmission electron microscope (FEI Tecnai G2). Briefly, s-Tmx-QT-SNEDDS (350 mg) was reconstituted with 50 ml of deionized water and allowed to stand for 15 min. The resultant emulsion was passed through the 0.22 μm membrane filter and allowed to stand for 2 h to attain the equilibrium. Diluted samples were negatively stained with 1% aqueous solution of phosphotungstic acid and visualized under the electron microscope after placing on 200-mesh carbon coated grids at 10–100 k-fold enlargements and accelerating voltage of 60.0 kV.

Antioxidant Activity

DPPH free radical scavenging assay was employed to evaluate the antioxidant activity of s-Tmx-QT SNEDDS (24). Stock

solution (1 μg/ml) of free drugs (Tmx and QT) and their combination (Tmx: QT 1:2 w/w) was prepared in methanol. s-Tmx-QT-SNEDDS was also mixed with methanol to completely extract the solubilized drugs. A 100 μl of methanolic solution of free drugs or drugs extracted from s-Tmx-QT-SNEDDS was mixed with 100 μl of DPPH (0.3 mM) reagent. The reaction mixture was incubated in dark at room temperature for 30 min and the absorbance of different samples was measured at 517 nm using microplate UV-spectrophotometer against control solution. The radical scavenging activity was calculated using the following equation:

$$\text{Scavanging activity}(\%) = \left(1 - \frac{A_{\text{sample}}}{A_{\text{control}}} \times 100\right)$$

Where A_{sample} and A_{control} is the absorbance of sample and control (QT solution), respectively. A calibration curve between % scavenging activity *vs*. amount of QT was also prepared by incubating the 100 μl of DPPH solution (0.3 mM) with 100 μl of QT solution containing the varying amount (0.5–5 μg of QT) using the same protocol as described above.

MCF-7 Cell Culture Experiments

Cell Culture

Human breast adenocarcinoma cells (MCF-7; American Type Culture Collection (ATCC) Manassas, VA, USA) were maintained in Minimum Essential Medium Eagle (MEM, Sigma) supplemented with Earle's salts, L-glutamine, non-essential amino acids, sodium bicarbonate, sodium pyruvate, 10% FBS, 100U/ml penicillin, and 100 μg/ml streptomycin (PAA Laboratories GmbH, Austria). The cells were grown at 37°C in 5% CO_2, and the culture medium was changed at every alternate day. After attaining the 90% confluency, cells were trypsinized with 0.25% trypsin-EDTA solution (Sigma, USA) and were further employed for cell uptake and cytotoxicity analysis of s-Tmx-QT-SNEDDS.

Cell Uptake and Intracellular Localization

MCF-7 cells were seeded at a density of 50,000 cells/well in 6 well culture plate (Costars, Corning Inc., NY, USA) for qualitative cell uptake analysis by the CLSM. Subsequent to cells reached the confluency, the medium was removed and cells were washed with Hank's Buffered Salt Solution (HBSS) (PAA Laboratories GmbH, Austria) for three times. Fluorescent s-Tmx-QT-SNEDDS (s-C6-Tmx-QT-SNEDDS) was prepared by solubilizing C-6 (1 mg) in liquid Tmx-QT-SNEDDS followed by the lyophilization using the previously described protocol. s-C6-Tmx-QT-SNEDDS was suitably reconstituted with deionized water and allowed to stand for 15 min and finally passed through the 0.22 μm membrane filter to obtain diluted C6-Tmx-QT-SNEDDS. MCF-7 cells were incubated with reconstituted C6-Tmx-QT-SNEDDS (equivalent 1 μg/ml to free C-6) for 1 h followed by fixing with 3% paraformaldehyde (Merck, India) and permeabilized with 0.2% Triton X-100. The nuclei of the cells were stained with 10 μg/ml DAPI (Sigma, USA). The cells were observed under the confocal laser scanning microscope (CLSM) (Olympus FV1000).

Quantitative Cell Uptake

MCF-7 cells were seeded at a density of 1,00,000 cells/well in 24 well cell culture plates (Costars, Corning Inc., NY, USA) and allowed to attach overnight. For evaluating the concentration dependent effect, MCF-7 cells were incubated with fresh medium containing varying concentration of free Tmx, QT, mixture of free Tmx with QT (1:2 w/w) and s-Tmx-QT-SNEDDS diluted with culture medium and further incubated for 1 h. Similarly, time dependent cell uptake was also evaluated by incubating MCF-7 cells with appropriate concentration of different formulations for varying time intervals (0.5, 1, 1.5, 2 h). Further, cells were lysed with 0.1% w/v Triton X-100 followed by extraction with methanol to completely solubilize the internalized drug. The cell lysate was centrifuged at 21,000 rpm for 10 min and obtained supernatant was subjected to HPLC analysis for quantification of internalized drugs.

Cell Cytotoxicity

MCF-7 cells were seeded at a density of 10,000 cells/well in 96 well cell culture plates (Costars, Corning Inc., NY, USA) and allowed to attach overnight. Following the cell attachment, media was replaced with fresh media containing free Tmx, QT, and mixture of free Tmx+ QT (1:2 w/w) and diluted s-Tmx-QT-SNEDDS so as to achieve the net concentration of 0.01, 0.1, 1 and 10 μg/ml (equivalent to free Tmx) and incubated for 6, 12 and 24 h. Additionally, s-Tmx-SNEDDS and s-QT-SNEDDS was also prepared using the same method as described in the previous section. Both the formulations were diluted with the fresh culture medium and further incubated with MCF-7 cells as to achieve the net concentration of 0.01, 0.1, 1 and 10 μg/ml (equivalent to free Tmx) and incubated for 6, 12 and 24 h. Upon completion of all the incubation period, the medium containing formulation was aspirated and cells were washed with phosphate buffer saline (PBS; pH 7.4). Subsequently, 150 μl of MTT solution (500 μg/ml in PBS) was added to each well and re-incubated for 3–4 h to facilitate formation of formazan crystals. The excess solution was then aspirated carefully and MTT formazan were dissolved in 200 μl of DMSO. The absorbance of the resultant solution was then measured at

550 nm using an ELISA plate reader (BioTek, USA). Cell viability was assessed using following formula:

$$Cell\ \ viability(\%) = \frac{A_{test} - A_{blank}}{A_{control} - A_{blank}} \times 100$$

Where A_{test}, A_{blank} and $A_{control}$ are absorbance of test, blank and control samples, respectively.

Median Effect Analysis

The results of *in vitro* cell cytotoxicity were further subjected to median effect analysis to evaluate the interaction between Tmx and QT formulations (39). Briefly, CalcuSyn software 2.1 (Biosoft, Ferguson, MO) was employed to generate the median effect plots between logarithm of drug dose (log D) and logarithm ratio of fraction of cells affected to unaffected (log f_a/f_u). Sigmoidicity of the dose–response curve (m) and D_m (median effect dose at which 50% cells are inhibited) was calculated from median effect plots. Assessment of synergistic effect, additive effect or antagonistic effect between different ratio of free drugs and drug nanoparticles was carried out based on combination index (CI) and dose reduction index (DRI) which were calculated by Calcusyn Software. CI value <1, $=1$ and >1 represent synergism, additive effect and antagonism, respectively (39).

In Vivo Pharmacokinetics

Animals and Dosing

All the animal studies protocols were duly approved by the Institutional Animal Ethics Committee (IAEC), NIPER, India. Female Sprague Dawley (SD) rats of 200–250 g were supplied by the central animal facility, NIPER, India. Animals were acclimatized at temperature of 25 ± 2°C and relative humidity of 50–60% under natural light/dark conditions for 1 week before experiments. The animals were randomly distributed into three groups each containing 6 animals. Different group of animals received oral Tmx citrate (10 mg/kg) and Tmx citrate (10 mg/Kg) in combination with QT (20 mg/Kg) and s-Tmx-QT-SNEDDS formulation (equivalent to 10 mg/kg of free Tmx). The blood samples (approximately 0.3 ml) were collected at predetermined time interval from the retro-orbital plexus under mild anesthesia into heparinized microcentrifuge tubes (containing 20 µl of 1,000 IU heparin/ml of blood). After each sampling, 1 ml of dextrose–normal saline was administered orally to prevent changes in the central compartment volume and electrolytes. Plasma was separated by centrifuging the blood samples at 10,000 rpm for 10 min at 4°C and kept at −80°C until analyzed.

Analysis of Tmx and QT in Plasma Samples

Plasma samples (250 µl) were mixed with 50 µl of internal standard (1-amino 4-nitro naphthalene; 2.5 µg/ml) and vortexed for 10 min. Subsequently, precipitation of plasma proteins was carried out by the addition of 800 µl of acetonitrile followed by vortexing for 15 min. The mixtures were centrifuged at 21,000 rpm for 10 min; supernatant was collected and dried in the vacuum centrifuge (Centri Vac, Inc. USA). Drug was extracted by addition of 100 µl methanol followed by vortexing for 10 min and then centrifugation at 10,000 rpm for 5 min. The amount of drugs in supernatants was analyzed by validated HPLC method. Briefly, 80 µl sample was injected into Shimadzu HPLC system equipped with Symmetry RP-18 column and SPD M-20A detector. Mobile phase employed for analysis was the mixture of acetonitrile, 10 mM ammonium acetate buffer and methanol (32:48:20 v/v).

Pharmacokinetics Data Analysis

The pharmacokinetic analysis of plasma concentration–time data was carried out by one compartmental model, using Kinetica-software (Thermo scientific). Required pharmacokinetics parameters like total area under the curve (AUC) $_{0\text{-}\infty}$, peak plasma concentration (C_{max}) and time to reach the maximum plasma concentration (T_{max}) were determined.

In Vivo Antitumor Efficacy

Antitumor efficacy of s-Tmx-QT-SNEDDS, free drugs and their combination was evaluated in breast tumor bearing animals. Tumor was induced by oral administration of 7, 12-dimethyl[α] benzanthracene (DMBA) solution (in soybean oil) to female SD rats (200–230 g) at the dose of 45 mg/kg at weekly interval for three consecutive weeks (4,40). Tumor bearing animals were separated and randomly divided into 4 treatment groups. During the study, tumor width (w) and length (l) were recorded with an electronic digital caliper and tumor size was calculated using the formula ($l \times W^2/2$). Drug treatment was started after the 10 weeks of the last does of DMBA administered. Animals were treated with the repeated oral dose (once in 3 days) of free Tmx citrate (3 mg/kg), combination of free Tmx citrate with free QT (1:2 w/w) (3 mg/kg free Tmx citrate and 6 mg/kg QT) and s-Tmx-QT-SNEDDS (3 mg/kg equivalent to Tmx). The positive control group received same repetitive oral administration of saline solution. Tumor growth was monitored for 30 days and the animals were euthanized. Survival of the animals was also monitored in another group of animals for 60 days.

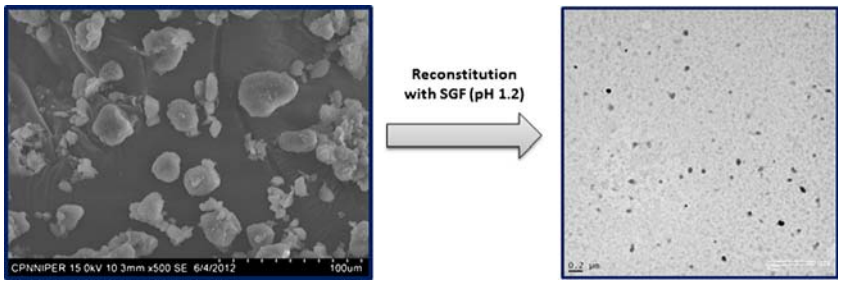

Fig. 1 Representative (**a**) SEM photograph of s-Tmx-QT-SNEDDS and (**b**) TEM photograph of nanoemulsion upon reconstitution of s-Tmx-QT-SNEDDS.

Evaluation of Angiogenesis Markers

After the completion of tumor inhibition study, animals were humanely sacrificed and blood was collected by the cardiac puncture in the heparinized centrifuge tubes. The plasma was separated by centrifuging the blood samples at 3,000 rcf for 5 min and stored at −20°C until analyzed. The levels of matrix metalloproteinases-2 (MMP-2) and metalloproteinases-9 (MMP-9) in plasma after completion of tumor inhibition studies were estimated by enzyme-linked immunoassay (ELISA) method by using the commercially available diagnostic kits (Cusabio Pvt. Ltd., China). Plasma collected from the healthy animals served as the negative control and was employed to normalize the MMP-2 and MMP-9 levels.

Hepatotoxicity

The levels of different hepatotoxicity markers such as Aspartate Aminotransferase (AST) and Alanine Aminotransferase (ALT) were also estimated in collected plasma by the commercially available kits (Accurex, Biomedical Pvt. Ltd.). In addition, whole liver was excised from all the animals and a representative part of liver tissue was fixed in neutral buffered formalin solution (10% v/v) and subjected for the routine histopathological examination (paraffin embedded specimen were cut into 5 μm sections and stained with hematoxylin and eosin). The remaining part of liver tissue was further homogenized in 5 volume of PBS (pH 7.4). The liver homogenate was employed for the determination of Thiobarbituric acid reactive substances (TBARS) and Glutathione (GSH) level using the commercially available diagnostic kits (Accurex Biomedical Pvt. Ltd., India), using the manufacturer's instructions.

Statistical Analysis

All *in vitro* and *in vivo* data are expressed as mean ± standard deviation (SD) and mean ± standard error of mean (SEM), respectively. Statistical analysis was performed with Sigma Stat (Version 2.03) using one-way ANOVA followed by Tukey–Kramer multiple comparison test. $P<0.05$ was considered as statistically significant difference.

RESULTS

Preparation and Characterization of s-Tmx-QT-SNEDDS

s-Tmx-QT-SNEDDS was prepared by lyophilization of liquid Tmx-QT-SNEDDS in the presence of Aerosil 200 as the solid carrier. Upon reconstitution, s-Tmx-QT-SNEDDS readily (in <2 min) resulted into nanoemulsion with smaller droplet size (82.12 ± 3.78 nm) and narrow PDI (0.162 ± 0.058). Further, s-Tmx-QT-SNEDDS was found to robust at all the dilutions and retained all the quality attributes upon reconstitution with simulated gastrointestinal fluids for the stipulated period.

Transmission Electron Microscopy (TEM) Upon Reconstitution

A TEM photograph of nanoemulsion obtained upon reconstitution of s-Tmx-QT-SNEDDS with deionized water is shown in Fig. 1, which showed spherical droplets. A good correlation was observed in droplet size measured by zeta sizer and TEM.

Free Radical Scavenging Activity

Figure 2 shows the free radical scavenging activity of free drugs, their combination and s-Tmx-QT-SNEDDS. An insignificant difference in free radical scavenging activity was observed between free QT and its combination with free Tmx. Free radical scavenging activity of the combination was maintained even after encapsulation in s-Tmx-QT-SNEDDS.

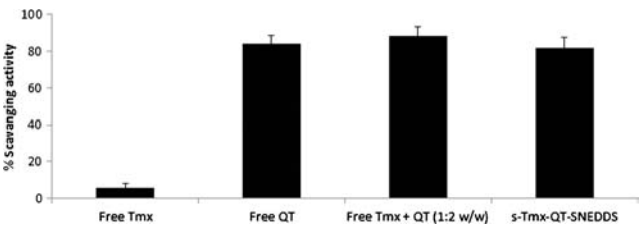

Fig. 2 Scavenging activity (%) of free drug, free drug mixture and s-Tmx-QT-SNEDDS. Each data point represents mean ± SD ($n=6$).

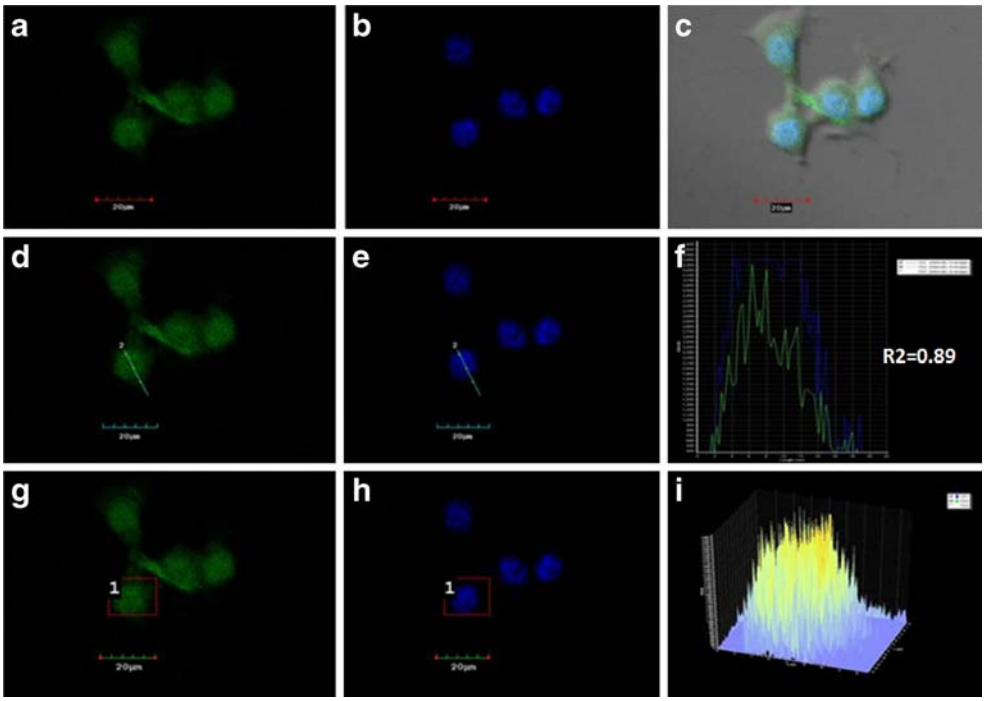

Fig. 3 Cell uptake and nuclear localization of s-C6-Tmx-QT-SNEDDS. (**a**) Uptake of SNEDDS by MCF-7 cells. (**b**) Nucleus stained by DAPI (**c**) Overlap image of (**a**, **b**). (**d**, **e**) 2-D line series analysis of fluorescence. (**f**) Line plot analysis of fluorescence. (**g**, **h**) 3-D Box analysis of the fluorescence. (**i**) 3-D box plot of fluorescence showing co-localization of green and blue fluorescence.

MCF-7 Cell Culture Experiments

Cell Uptake and Intracellular Localization

The cellular uptake of C-6-Tmx-QT-SNEDDS was evident within 1 h of incubation with MCF-7 cells (Fig. 3a). C-6-Tmx-QT-SNEDDS showed significant localization with the nucleus of MCF-7 cells, as confirmed by overlaying the green and blue fluorescence of C-6 and DAPI, respectively (Fig. 3c). The nuclear localization of the C6-Tmx-QT-SNEDDS was further endorsed by the 2-D line series (Fig. 3d–f) and 3-D box analysis (Fig. 3g–i) of the cells. Nearly 90% (Pierson's coefficient = 0.89) of the green fluorescence (C-6) was co-localized with the blue fluorescence (DAPI) (Fig. 3f) indicating rapid internalization and nuclear transport of C6-Tmx-QT-SNEDDS.

Quantitative Cell Uptake Studies

Concentration and time dependent cell uptake of Tmx and QT by MCF-7 cells was observed upon incubation with free Tmx, QT, their combination (1:2 w/w) and s-Tmx-QT-SNEDDS (Fig. 4). Significantly higher ($p < 0.001$) steady state concentration of both the drugs in lesser time (Tmx 6.23 ± 0.52 μg/ml; QT 13.05 ± 0.82 μg/ml at 1 h) was observed in case of s-Tmx-QT-SNEDDS in comparison with free Tmx (0.121 ± 0.08 μg/ml; 2 h), QT (1.58 ± 0.09 μg/ml; 2 h) and their combination (Tmx 0.229 ± 0.01 μg/ml; QT 1.56 ±

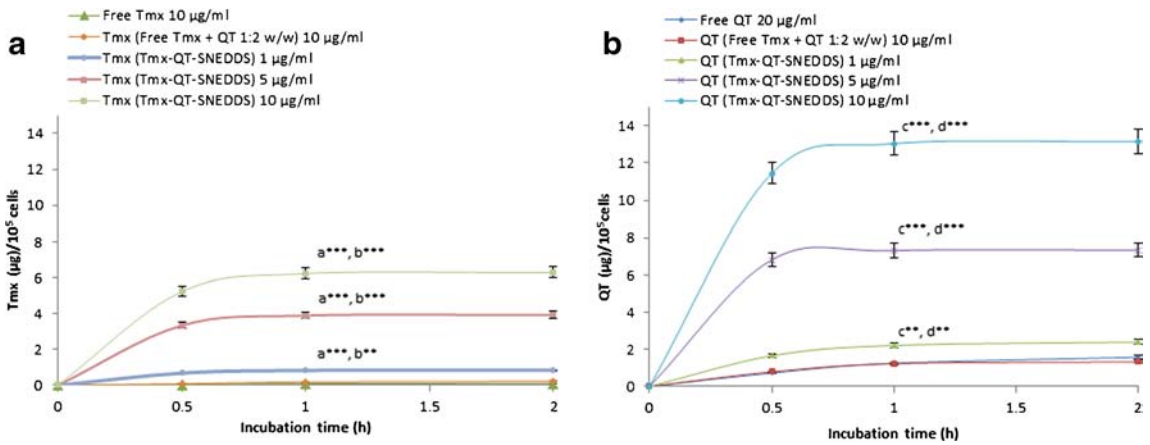

Fig. 4 Time and concentration dependent uptake profile of Tmx (**a**) and QT (**b**) upon incubation with free Tmx, QT, mixture of Tmx and QT (1:2 w/w) and s-Tmx-QT-SNEDDS with the MCF-7 cells. Each data point represents mean ± SD ($n = 4$).

0.08 μg/ml; 2 h). Upon comparing the data of 1 h incubation time, s-Tmx-QT-SNEDDS revealed ~63-fold and ~33-fold increase in cellular uptake of Tmx in contrast to free Tmx and its combination with QT (1:2 w/w). Similarly, ~10-fold appreciation in the cell uptake of QT was also observed in case of s-Tmx-QT-SNEDDS in contrast to free QT as well as its combination with free Tmx.

Cell Cytotoxicity

Concentration and time dependent cell viability of free drugs, their combination (free Tmx+ QT 1:2 w/w) and s-Tmx-QT-SNEDDS are shown in Fig. 5. All the formulations revealed concentration and time dependent increase in cytotoxicity against MCF-7 cells, whereas >95% cell viability was observed in case of blank SNEDDS formulation at all the incubation times. Further, s-Tmx-QT-SNEDDS revealed significantly higher cytotoxicity in comparison with free drug combination ($p < 0.05$) as well as individual free drugs ($p < 0.001$). At 24 h, s-Tmx-QT-SNEDDS revealed ~47-fold and ~6-fold increase in the cell cytotoxicity as compared to free Tmx and free Tmx+ QT (1:2 w/w), respectively (Table I). Table II depicts the time and concentration dependent dose reduction index (DRI) of Tmx and QT upon incubation of MCF-7 cells with free drug combination and s-Tmx-QT-SNEDDS. A significantly higher DRI value of both the drugs was found in case of s-Tmx-QT-SNEDDS in comparison with free drug combination. However, combination index (CI) was found to be <1 in case of free drug combination and s-Tmx-QT-SEDDS at all the concentration and incubation time (see Supplementary Material Table SI). The highest DRI of 32.86- and 22.25-fold was observed in case of s-Tmx-QT-SNEDDS, while in case of free drug combination DRI was found to be only 5.94- and 3.82-fold for Tmx and QT respectively.

In Vivo Pharmacokinetics

The plasma concentration-time profiles after single oral administration of the s-Tmx-QT-SNEDDS, free Tmx-citrate and its combination with free QT are shown in Fig. 6. Various pharmacokinetic parameters estimated with one compartment model analysis of plasma concentration data are summarized in Table III. Co-administration of QT along with free Tmx citrate resulted into 1.66-fold and 1.97-fold enhancement in C_{max} and $AUC_{0-\infty}$ of Tmx, respectively, whereas the same parameters for QT remained unaffected ($p > 0.05$) upon co-administration with Tmx. Interestingly, s-Tmx-QT-SNEDDS led to 8.04- and 4.07-fold enhancement in the $AUC_{0-\infty}$ as compared to free Tmx-citrate alone and co-administered with free QT, respectively. In addition, QT bioavailability was also increased by ~3.9-fold from s-Tmx-QT-SNEDDS in comparison with free QT or its combination with free Tmx.

Table I IC_{50} Dose of Free Tmx, Free QT and Combination of Free Tmx With QT and s-Tmx-QT-SNEDDS Upon Treatment With MCF-7 Cells

Formulations	IC_{50} value (μg/ml)		
	6 h	12 h	24 h
Free Tmx	174.06 ± 9.70	115.54 ± 6.77	47.06 ± 2.3
Free QT	254.32 ± 15.71	121.69 ± 8.08	62.04 ± 3.10
Free Tmx + QT (1:2)	42.07 ± 3.20	23.31 ± 2.16	6.37 ± 2.31
s-Tmx-QT-SNEDDS	28.63 ± 2.43	5.95 ± 0.29	1.13 ± 0.05

[a] Data are expressed as mean ± SD ($n = 4$), ***$p < 0.001$, **$p < 0.01$; a *vs*. free Tmx, b *vs*. free QT, c *vs*. free Tmx+ QT (1:2 w/w)

In Vivo Antitumor Efficacy

Figure 7 shows the *in vivo* antitumor efficacy after repetitive oral administration of free Tmx (3 mg/kg), free Tmx+ QT (1:2 w/w) (3 mg/kg; 6 mg/kg QT) and s-Tmx-QT-SNEDDS (3 mg/kg equivalent to Tmx citrate) for 30 days. Tumor growth progression clearly indicates that all the formulation significantly inhibited the tumor volume in comparison with control group of animals (DMBA treated) (Fig. 7a). Co-administration of free QT along with Tmx citrate resulted into suppression of tumor growth but found to be insignificant ($p > 0.05$) when compared with that of Tmx citrate treated animals. Notably, significant suppression in the tumor growth was observed in case of s-Tmx-QT-SNEDDS in comparison with both free Tmx citrate and its combination with QT. After

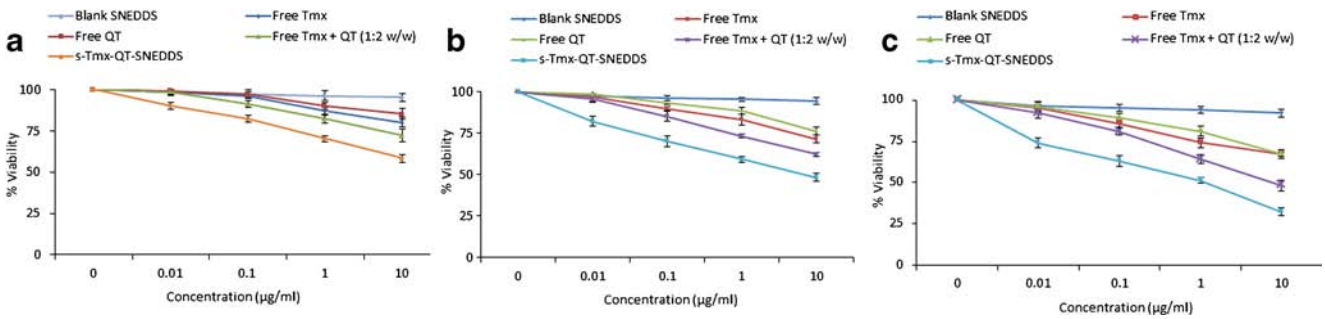

Fig. 5 Cell cytotoxicity of free Tmx, free QT, combination of free Tmx and QT (1:2) and s-Tmx-QT-SNEDDS (**a**) after 6 h (**b**) after 12 h (**c**) after 24 h. Each data point represented as mean ± SD ($n = 4$).

Table II Dose Reduction Index of Tmx and QT After Treatment of MCF-7 Cells With Free Tmx+ QT (1:2 w/w) and s-Tmx-QT-SNEDDS

Incubation time (h)	Concentration (μg/ml)	Dose Reduction Index (DRI)			
		Free Tmx + QT (1:2 w/w)		s-Tmx-QT-SNEDDS	
		Tmx	QT	Tmx	QT
6 h*	0.01	0.874	1.381	4.929	5.899
	0.1	7.172	8.036	10.062	8.711
	1	4.896	4.724	12.623	10.327
	10	1.879	1.632	15.987	13.025
12 h*	0.01	1.428	4.273	7.038	6.288
	0.1	6.774	9.623	11.996	7.272
	1	6.026	5.613	12.432	12.036
	10	2.703	1.884	18.186	12.329
24 h*	0.01	2.553	3.13	14.234	10.147
	0.1	5.738	5.417	23.256	13.322
	1	7.992	6.049	30.043	16.189
	10	5.944	3.802	32.867	22.252

*Combination index in all the cases was < 1

the 30 days of study, the residual tumor burden was ~20% in case of s-Tmx-QT-SNEDDS, whereas animal group treated with combination drugs (free Tmx+ QT 1:2 w/w) and free Tmx citrate showed the residual tumor burden of ~57% and ~65% respectively (Fig. 7b). Figure 7c shows the representative photographs of tumor excised from untreated and animals treated with different formulations. Kaplan-Mirer survival plots of animals after 60 days repetitive treatment with different formulation is shown in Fig. 8. No mortality throughout the study period was recorded in s-Tmx-QT-SNEDDS treated animal group, whereas 50% mortality was observed in the animal group treated with free Tmx citrate as well as combination of Tmx citrate +QT (1:2 w/w).

Evaluation of Tumor Angiogenesis Markers

Figure 9 shows the levels of MMP-2 and MMP-9 in plasma samples of animal group treated with different formulations for 30 days. Repetitive treatment of DMBA induced tumor bearing female SD rats with s-Tmx-QT-SNEDDS controlled the levels of both the tumor angiogenesis makers (MMP-2 and MMP-9), whereas significantly ($p < 0.05$) higher levels of both the markers were observed in case of free Tmx citrate or its combination with free QT.

Hepatotoxicity

Figure 10 depicts the levels of various hepatotoxicity markers estimated in plasma and liver tissue after 30 days treatment with different formulations. The animals treated with free Tmx citrate posed significantly ($p < 0.001$) higher level of AST, ALT in plasma (Fig. 10a and b) and TBARS level in liver tissue (Fig. 10c) as compared to control (healthy animals). Alongside, the level of GSH in liver homogenates was significantly decreased in case of free Tmx citrate treatment as compared to control group (Fig. 10d). No significant improvement in the levels of hepatotoxicity markers was observed upon co-administration of QT along with free Tmx citrate. The results were further corroborated by the histopathological examination of representative liver tissue following treatment with free Tmx citrate and its combination with free QT, which revealed marked parenchymal degeneration with heterochromatic nuclei (Fig. 11b–C). Interestingly, no significant change ($p > 0.05$) in the levels of all tested hepatotoxicity markers were observed in case of s-Tmx-QT-SNEDDS when compared to that of control (healthy animals). The results were also supported by the histopathological section of liver tissue treated with s-Tmx-QT-SNEDDS, revealing cellular architecture closely resembled with the control liver section (healthy animals).

DISCUSSION

The aim of the present study was to develop s-SNEDDS loaded with Tmx and QT in the clinically effective therapeutic dose for improved breast cancer efficacy and reduced hepatotoxicity of Tmx. With this goal in mind, previously

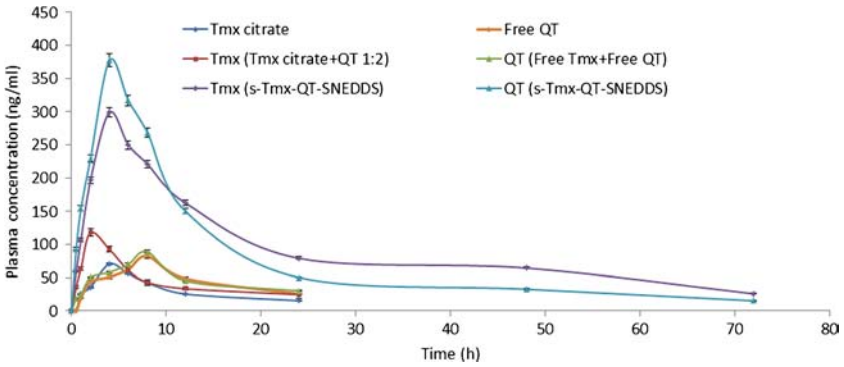

Fig. 6 Plasma concentration time profiles of Tmx after oral administration to SD rats at 10 mg/kg dose formulated in solid self-emulsifying formulation along with QT, compared with the oral administration of equivalent dose of Tmx citrate + QT and Tmx citrate (10 mg/Kg). Each data point represents mean ± SD ($n = 5$).

Table III Pharmacokinetics Parameters of s-Tmx-QT-SNEDDS and Free Drugs

Pharmacokinetics parameters	Free Tmx citrate	Free QT	Free Tmx citrate + free QT (1:2 w/w)		s-Tmx-QT-SNEDDS	
			Tmx	QT	Tmx	QT
$AUC_{0-\infty}$ (ng/ml.h)	931.39 ± 22.47	1641.17 ± 42.68	1837.98 ± 40.35	1650.34 ± 24.70	7494.13 ± 350.23	6420.14 ± 320.23
C_{max} (ng/ml)	70.71 ± 15.23	89.12 ± 1.23	118.06 ± 5.93	82.59 ± 6.23	299.13 ± 18.36	377.48 ± 23.56
T_{max} (h)	4	8	2	8	4	4

Data are expressed as mean ± SEM ($n = 5$)

developed s-Tmx-QT-SNEDDS was evaluated for *in vivo* pharmacokinetics, anticancer efficacy and hepatotoxicity.

The functional architecture of QT in SNEDDS has been recently endorsed by our group using DPPH assay and is also evident in present work revealing insignificant difference between free radical scavenging activity among free QT, free Tmx+ QT (1:2 w/w) and s-Tmx-QT-SNEDDS (24). Further, s-Tmx-QT-SNEDDS was evaluated for cell uptake and intracellular localization in MCF-7 cells to establish the proof of concept for synergistic cytotoxicity of the co-encapsulated drugs. As evident from Fig. 3, nanoemulsion droplets resulted from C-6-Tmx-QT-SNEDDS were efficiently internalized by MCF-7 cells within 1 h of incubation. The rationalized design of the developed formulation was based upon the concomitant delivery of Tmx and QT in the vicinity of nucleus of cancer cells, owing to the binding affinity of both the drugs with estrogen receptor in the nuclear region (22). The degree of nuclear localization was further confirmed by Pearson's correlation coefficient (r) that was found to be ~0.9 indicating very high degree (~90%) of overlap between the fluorescence of C-6 loaded SNEDDS and DAPI. As per our knowledge, this is the first report where we envisaged the significant nuclear localization of self-emulsifying formulation upon incubation with MCF-7 cells. It has been anticipated that surfactant stabilized oily droplets are efficiently internalized by MCF-7 cells and release both the drugs in the nuclear and peri-nuclear region which then bind with the estrogen receptor to elucidate the pharmacological effect. Quantitative analysis of cell uptake revealed significantly ($p < 0.001$) higher and rapid internalization within 1 h of incubation in contrast to respective free drugs or their combination, which showed maximum uptake after 2 h (Fig. 4). The promising findings of quantitative cell uptake were well corroborated by the observed cytotoxicity of the s-Tmx-QT-SNEDDS, which

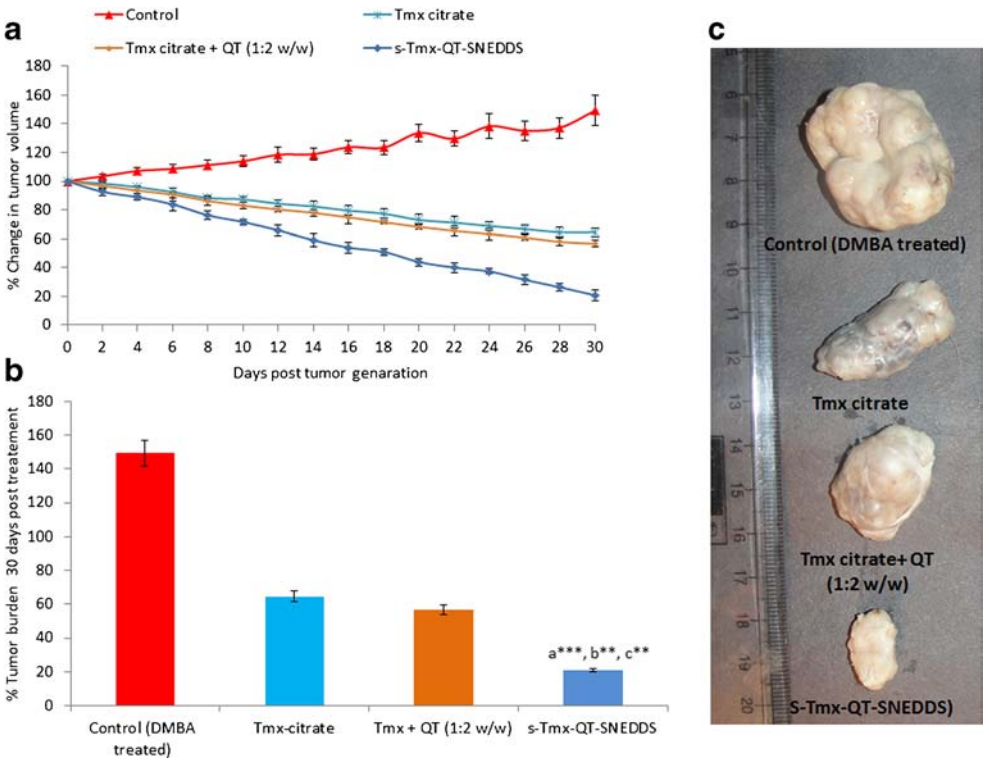

Fig. 7 *In vivo* antitumor efficacy in DMBA induced breast tumor female SD rats. (**a**) Tumor progression after repetitive oral administration of different formulations. (**b**) Residual tumor burden after 30 days. (**c**) Photographs of representative excised tumors tissue from animals treated with different formulations. Each data point represents mean ± SEM ($n = 8$).

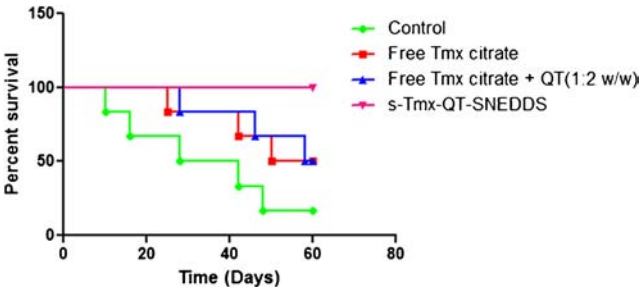

Fig. 8 Kaplan-Meier survival curve of tumor bearing rats treated with various Tmx formulations (3 mg/Kg equivalent to free Tmx).

revealed ~47-fold and ~6-fold appreciation in comparison with free Tmx and free Tmx+ QT (1:2 w/w), respectively (Table I). Surfactant stabilized oily droplets are rapidly internalized by fluid phase pinocytosis in contrast to free drugs which are mainly transported by the passive diffusion (2). However, ~8-fold appreciation in cell cytotoxicity of free drug combination (free Tmx+ QT 1:2 w/w) in comparison with free Tmx could be attributed to selective inhibition of P-gp efflux by QT, which also enhance the intracellular concentration of Tmx (41). Further, median effect analysis was employed to predict the time and concentration dependent dose response of the free drug combination and s-Tmx-QT-SNEDDS. The dose–response of s-Tmx-SNEDDS and s-QT-SNEDDS was also investigated to predict the dose response of s-Tmx-QT-SNEDDS (data not shown). Both the free drug combination and s-Tmx-QT-SNEDDS revealed combination index (CI) value <1, indicating the synergism between the said combinations at all the tested concentration and incubation time (39). The selective binding of both the drugs to the estrogen receptor, but at the dissimilar sites in the nucleus could explain the potential synergism between Tmx and QT (22). However, free drug combination revealed non-uniform and unpredictable pattern in DRI, which could be attributed to the dissimilar solubility profile and/or metabolism of QT. Interestingly, s-Tmx-QT-SNEDDS revealed significantly higher DRI in comparison with free drug combination, which could be attributed to their higher cell cytotoxicity as compared to free drug combination. Furthermore, it is anticipated that superior internalization of QT by SNEDDS may further inhibit the P-gp efflux of Tmx, thereby promoting its retention inside the MCF-7 cells (27). Moreover, a remarkably higher DRI (~32-fold) for Tmx in contrast to that of QT (~22-fold) reveals relatively higher contribution of QT to the overall efficacy of the formulation. The proportionate reduction in the dose of Tmx could be exploited to either improve upon therapeutic efficacy and/or reducing Tmx induced hepatotoxicity (39). In addition, the developed formulation owing to quite high DRI values pose potential pharmacoeconomic benefits.

Encouraged with our earlier findings of *in vitro* Caco-2 cell uptake studies, *in vivo* pharmacokinetics of s-Tmx-QT-SNEDDS was performed in female SD rats following oral administration. Approximately, 1.6-fold increase in C_{max} of Tmx upon co-administration with free QT might be due to selective inhibition of P-gp efflux pumps by QT leading to its increased oral bioavailability (42). Interestingly, peak plasma concentration (C_{max}) as well as $AUC_{0-\infty}$ of both the drugs (Tmx and QT) was significantly increased upon oral administration of s-Tmx-QT-SNEDDS. Immediate emulsification of s-Tmx-QT-SNEDDS in GI tract leads to increased dispersion of both the drugs at the site of absorption, thereby overcomes the barriers of solubility-limited absorption (37). As far as the previous literature is concerned, this is the first report, which demonstrates the enhanced oral bioavailability of dual drug via s-SNEDDS. About 8-fold and 4-fold increase in oral bioavailability of Tmx and QT as compared to respective free drugs, could be attributed to the preferential uptake of drug loaded oily droplets by the chylomicron assisted lymphatic absorption, thereby preventing the first pass metabolism of both the drugs (43). Of note, P-gp inhibition effect of QT may be additional reason for relatively higher increase in Tmx bioavailability in combination SNEDDS.

Bring into line of our previous experience on evaluation of various nanocarriers and encouraged from the results of *in vivo* pharmacokinetics, antitumor efficacy of s-Tmx-QT-SNEDDS was evaluated in DMBA induced

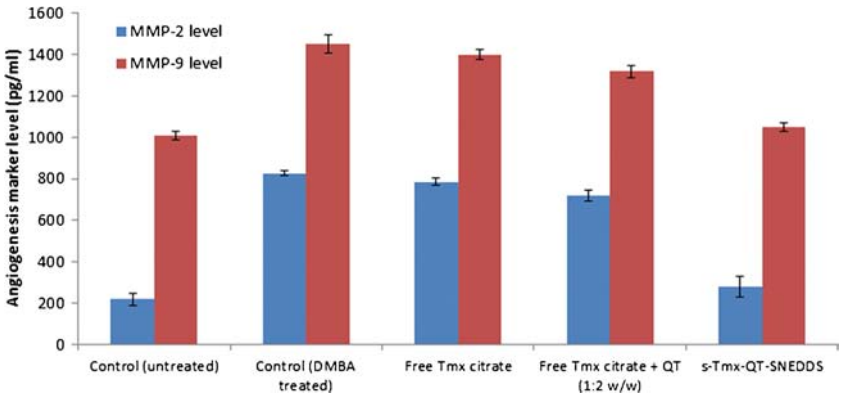

Fig. 9 Plasma levels of MMP-2 and MMP-9 after treatment with different formulations. Each data point represents mean ± SEM ($n = 6$).

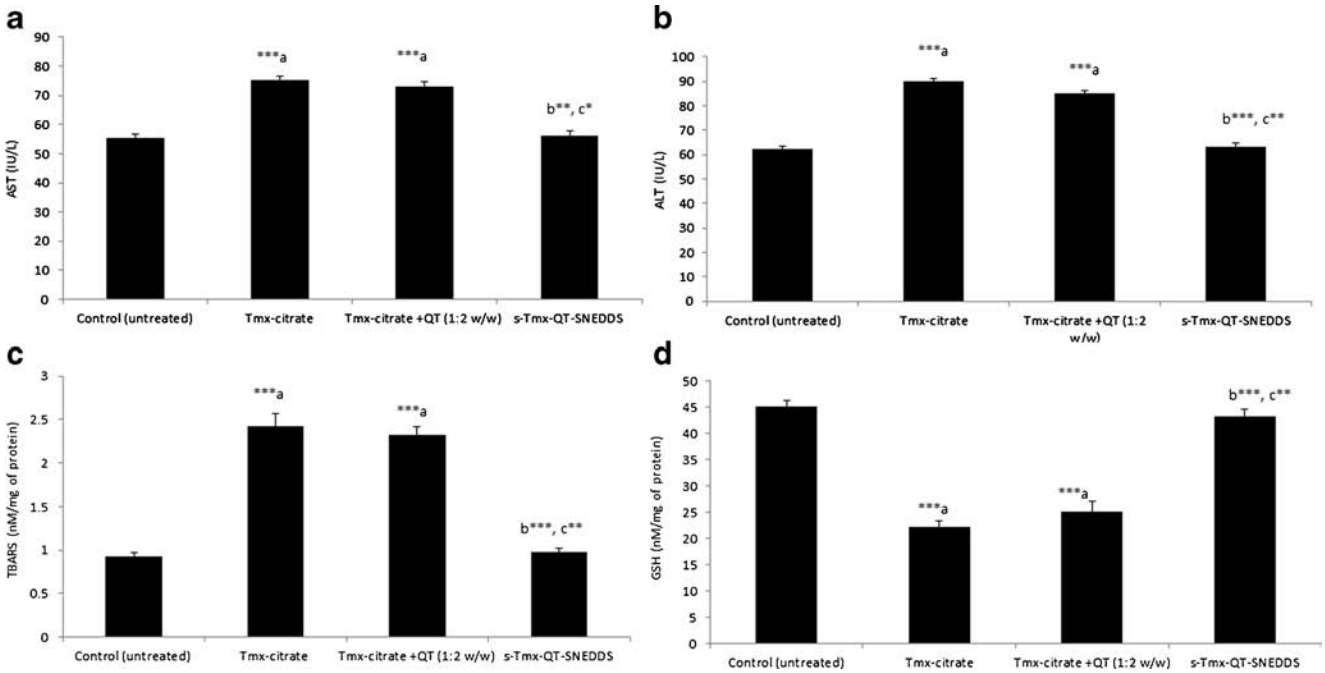

Fig. 10 Levels of different toxicity maker levels (**a**) AST (**b**) ALT (**c**) TBARS (**d**) GSH after treatment with different Tmx formulations. ***$p < 0.001$, **$p < 0.01$, *$p < 0.05$; a *vs*. control (untreated healthy animals), b *vs*. Tmx-citrate, c *vs*. Tmx citrate + QT (1:2 w/w). Each data point represents mean ± SEM ($n = 6$).

breast tumor female SD rats. Similar to free Tmx citrate, poor oral absorption of QT led to insignificant appreciation in tumor growth suppression in case of free drug combination (24). Interestingly, co-encapsulation of both the drugs in s-Tmx-QT-SNEDDS revealed ~80% suppression in tumor growth in contrast to free Tmx citrate and its combination with QT, which revealed ~35% and ~44% reduction in tumor volume, respectively. This might be due to the higher accumulation of both the drugs in tumor microenvironment via the precise transport of s-Tmx-QT-SNEDDS into the lymphatic vessels which is also present in tumor tissue in the form of rich network (44). The normalized levels of tumor angiogenesis markers (MMP-2, MMP-9) further endorsed the augmented antitumor efficacy of s-Tmx-QT-SNEDDS (Fig. 9). Increased levels of matrix metalloproteinase (MMP-2 and MMP-9), a large family of zinc-dependent endopeptidases, are usually associated with tumor angiogenesis, growth of cancer cells and their differentiation (45). Apart from multiple cellular mechanism, QT also has a propensity to control the levels of matrix metalloproteinase, thus prevents the tumor angiogenesis and progression (46). Present findings are in line with the report of Ma and co-workers, which revealed reduced degree of angiogenesis by combination of Tmx and QT (46). However, in our case combination of free Tmx+ QT (1:2 w/w) did not normalize the levels of both the angiogenesis markers, when compared to the untreated animals (DMBA treated). Interestingly, s-Tmx-QT-SNEDDS efficiently controlled the levels of both the tumor angiogenesis markers, which might be due to significant appreciation in oral bioavailability of both the drugs.

With significant improvement in the bioavailability and antitumor efficacy of s-Tmx-QT-SNEDDS, Tmx induced hepatotoxicity was evaluated by estimating the levels of hepatotoxicity markers (Fig. 10) and histopathological examinations (Fig. 11). Our findings are in line with our previous studies which suggested that repetitive oral administration of Tmx citrate leads to hepatotoxicity as indicated by the levels of various hepatotoxicity markers as well as histological changes in liver tissue (4). In our recent report, we attempted to co-encapsulate the QT along with Tmx in PLGA-NPs and

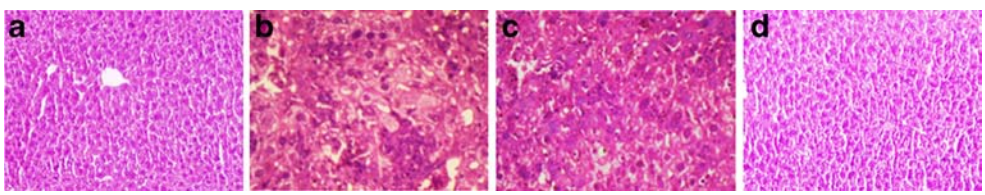

Fig. 11 Histological examination of liver after treatment with different formulations. (**a**) Untreated (Healthy animals), (**b**) Tmx citrate, (**c**) Tmx citrate + free QT (1:2 w/w), (**d**) s-Tmx-QT-SNEDDS.

found complete obliteration in the Tmx induced hepatotoxicity [1]. Similar findings were also observed in case of s-Tmx-QT-SNEDDS, where all the hepatotoxicity markers were normalized to control level (healthy animals). Generally, ability to bypass the hepatic metabolism vis-à-vis maintained plasma level of antioxidant i.e. QT could be attributed to complete abolishment in Tmx induced hepatotoxicity in case of s-Tmx-QT-SNEDDS.

CONCLUSION

Present investigation reports a novel solid self-nanoemulsifying formulation for oral delivery of clinically relevant therapeutic combination (Tmx and QT) for the effective treatment of breast cancer. The formulation was developed utilizing GRAS listed excipients in the quantity well below their IIG limits. The manufacturing process being mere mixing of ingredients posed high level of manufacturing scalability and industrial adaptability. Co-formulation of antioxidant i.e. QT along with Tmx in single nanocarriers system resulted into significant appreciation in anticancer efficacy as compared to commercially available Tmx-citrate. The developed formulation also revealed its potential to completely abolish the Tmx induced hepatotoxicity, which could be great clinical relevance. Further, the tissue bio-distribution and multiple dose kinetics could be evaluated for better understanding of developed formulation for synchronous delivery of co-encapsulated drugs.

ACKNOWLEDGMENTS AND DISCLOSURES

The authors are thankful to Director, NIPER for providing the necessary infrastructure and facilities and Department of Science & Technology (DST), Government of India, New Delhi, and financial support. A.K.J and K.T. are grateful to Council of Scientific and Industrial Research (CSIR), GoI, New Delhi, for providing research fellowships. Histopathological examination carried out at the Medicos Lab, Chandigarh, India is also duly acknowledged.

REFERENCES

1. Jain AK, Thanki K, Jain S. Co-encapsulation of tamoxifen and quercetin in polymeric nanoparticles: implications on oral Bioavailability, antitumor efficacy, and drug-Induced toxicity. Mol Pharmaceutics. 2013. doi:10.1021/mp400311j.
2. Thanki K, Gangawal RP, Sangamwar AT, Jain S. Oral delivery of anticancer drugs: challenges and opportunities. J Control Rel. 2013;170(1):15–40.
3. Jordan VC. Tamoxifen: a most unlikely pioneering medicine. Nat Rev Drug Discov. 2003;2(3):205–13.
4. Jain AK, Swarnakar NK, Godugu C, Singh RP, Jain S. The effect of the oral administration of polymeric nanoparticles on the efficacy and toxicity of tamoxifen. Biomaterials. 2012;32(2):503–15.
5. Lettéron P, Labbe G, Degott C, Berson A, Fromenty B, Delaforge M, *et al*. Mechanism for the protective effects of silymarin against carbon tetrachloride-induced lipid peroxidation and hepatotoxicity in mice: evidence that silymarin acts both as an inhibitor of metabolic activation and as a chain-breaking antioxidant. Biochem Pharmacol. 1990;39(12):2027–34.
6. McVie JG, Simonetti GP, Stevenson D, Briggs RJ, Guelen PJ, de Vos D. The bioavailability of Tamoplex (tamoxifen). Part 1. A pilot study. Methods Find Exp Clin Pharmacol. 1986;8(8):505–12.
7. Tukker JJ, Blankenstein MA, Nortier JW. Comparison of bioavailability in man of tamoxifen after oral and rectal administration. J Pharm Pharmacol. 1986;38(12):888–92.
8. Middleton E, Kandaswami C, Theoharides TC. The effects of plant flavonoids on mammalian cells: implications for inflammation, heart disease, and cancer. Pharmacol Rev. 2000;52(4):673–751.
9. Boots AW, Haenen G, Bast A. Health effects of quercetin: from antioxidant to nutraceutical. Eur J Pharmacol. 2008;585(2–3):325–37.
10. Piantelli M, Maggiano N, Ricci R, Larocca LM, Capelli A, Scambia G, *et al*. Tamoxifen and quercetin interact with type II estrogen binding sites and inhibit the growth of human melanoma cells. J Invest Dermatol. 1995;105(2):248–53.
11. Caltagirone S, Rossi C, Poggi A, Ranelletti FO, Natali PG, Brunetti M, *et al*. Flavonoids apigenin and quercetin inhibit melanoma growth and metastatic potential. Int J Cancer. 2000;87(4):595–600.
12. Sartippour MR, Pietras R, Marquez-Garban DC, Chen HW, Heber D, Henning SM, *et al*. The combination of green tea and tamoxifen is effective against breast cancer. Carcinogenesis. 2006;27(12):2424–33.
13. Ma ZS, Thanh HOAH, Chee Pang NG, Phuc Tien DO, Thanh HN, Hung H. Reduction of CWR22 prostate tumor xenograft growth by combined tamoxifen-quercetin treatment is associated with inhibition of angiogenesis and cellular proliferation. Int J Oncol. 2004;24(5):1297–304.
14. Brookes PS, Digerness SB, Parks DA, Darley-Usmar V. Mitochondrial function in response to cardiac ischemia-reperfusion after oral treatment with quercetin. Free Radic Biol Med. 2002;32(11):1220–8.
15. Liu S, Hou W, Yao P, Li N, Zhang B, Hao L, *et al*. Heme oxygenase-1 mediates the protective role of quercetin against ethanol-induced rat hepatocytes oxidative damage. Toxicol In Vitro. 2012;26(1):74–80.
16. Gupta C, Vikram A, Tripathi DN, Ramarao P, Jena GB. Antioxidant and antimutagenic effect of quercetin against DEN induced hepatotoxicity in rat. Phytother Res. 2010;24(1):119–28.
17. Abo-Salem OM, Abd-Ellah MF, Ghonaim MM. Hepatoprotective activity of quercetin against acrylonitrile induced hepatotoxicity in rats. J Biochem Mol Toxicol. 2011;25(6):386–92.
18. Tabassum H, Parvez S, Rehman H, Banerjee BD, Raisuddin S. Catechin as an antioxidant in liver mitochondrial toxicity: inhibition of tamoxifen induced protein oxidation and lipid peroxidation. J Biochem Mol Toxicol. 2007;21(3):110–7.
19. Granado-Serrano AB, Martin MA, Bravo L, Goya L, Ramos S. Quercetin induces apoptosis via caspase activation, regulation of Bcl-2, and inhibition of PI-3-kinase/Akt and ERK pathways in a human hepatoma cell line (HepG2). J Nutr. 2006;136(11):2715–21.
20. Caltagirone S, Ranelletti FO, Rinelli A, Maggiano N, Colasante A, Musiani P, *et al*. Interaction with type II estrogen binding sites and antiproliferative activity of tamoxifen and quercetin in human non-small-cell lung cancer. Am J Respir Cell Mol Biol. 1997;17(1):51–9.
21. Ma ZS, Huynh TH, Ng CP, Do PT, Nguyen TH, Huynh H. Reduction of CWR22 prostate tumor xenograft growth by combined tamoxifen-quercetin treatment is associated with inhibition of angiogenesis and cellular proliferation. Int J Oncol. 2004;24(5):1297–304.
22. Lama G, Angelucci C, Bruzzese N, Nori SL, D'Atri S, Turriziani M, *et al*. Sensitivity of human melanoma cells to oestrogens, tamoxifen

and quercetin: is there any relationship with type I and II oestrogen binding site expression? Melanoma Res. 1998;8(4):313–22.
23. Date AA, Nagarsenker MS, Patere S, Dhawan V, Gude RP, Hassan PA, *et al*. Lecithin-based novel cationic nanocarriers (Leciplex) II: improving therapeutic efficacy of quercetin on oral administration. Mol Pharmaceutics. 2011;8(3):716–26.
24. Jain S, Jain AK, Pohekar M, Thanki K. Novel self-emulsifying formulation of quercetin for improved in vivo antioxidant potential: implications on drug induced cardiotoxicity and nephrotoxicity. Free Radic Biol Med. 2013;65C:117–30.
25. Zhigaltsev IV, Maurer N, Akhong Q-F, Leone R, Leng E, Wang J, *et al*. Liposome-encapsulated vincristine, vinblastine and vinorelbine: a comparative study of drug loading and retention. J Control Rel. 2005;104(1):103–11.
26. Bayne WF, Mayer LD, Swenson CE. Pharmacokinetics of CPX–351 (cytarabine/daunorubicin HCl) liposome injection in the mouse. J Pharm Sci. 2009;98(7):2540–8.
27. Misra R, Sahoo SK. Coformulation of doxorubicin and curcumin in poly (D, L-lactide-co-glycolide) nanoparticles suppresses the development of multidrug resistance in K562 cells. Mol Pharmaceutics. 2011;8(3):852–66.
28. Acharya S, Sahoo SK. Sustained targeting of Bcr–Abl+ leukemia cells by synergistic action of dual drug loaded nanoparticles and its implication for leukemia therapy. Biomaterials. 2011;32(24): 5643–62.
29. Zhang L, Radovic–Moreno AF, Alexis F, Gu FX, Basto PA, Bagalkot V, *et al*. Co–delivery of hydrophobic and hydrophilic drugs from nanoparticle–aptamer bioconjugates. Chemmedchem. 2007;2(9): 1268–71.
30. Song XR, Cai Z, Zheng Y, He G, Cui FY, Gong DQ, *et al*. Reversion of multidrug resistance by co-encapsulation of vincristine and verapamil in PLGA nanoparticles. Eur J Pharm Sci. 2009;37(3):300–5.
31. Lammers T, Subr V, Ulbrich K, Peschke P, Huber PE, Hennink WE, *et al*. Simultaneous delivery of doxorubicin and gemcitabine to tumors in vivo using prototypic polymeric drug carriers. Biomaterials. 2009;30(20):3466–75.
32. Krakovičová H, Etrych T, Ulbrich K. HPMA-based polymer conjugates with drug combination. Eur J Pharm Sci. 2009;37(3): 405–12.
33. Chen AM, Zhang M, Wei D, Stueber D, Taratula O, Minko T, *et al*. Co–delivery of doxorubicin and Bcl–2 siRNA by mesoporous silica nanoparticles enhances the efficacy of chemotherapy in multidrug–resistant cancer cells. Small. 2009;5(23):2673–7.
34. Kaneshiro TL, Lu Z-R. Targeted intracellular codelivery of chemotherapeutics and nucleic acid with a well-defined dendrimer-based nanoglobular carrier. Biomaterials. 2009;30(29):5660–6.
35. Pouton CW. Formulation of self-emulsifying drug delivery systems. Adv Drug Deliv Rev. 1997;25(1):47–58.
36. Neslihan Gursoy R, Benita S. Self-emulsifying drug delivery systems (SEDDS) for improved oral delivery of lipophilic drugs. Biomed Pharmacother. 2004;58(3):173–82.
37. Tang B, Cheng G, Gu JC, Xu CH. Development of solid self-emulsifying drug delivery systems: preparation techniques and dosage forms. Drug Discov Today. 2008;13(13):606–12.
38. Jain S, Chauhan DS, Jain AK, Swarnakar NK, Harde H, Mahajan RR, *et al*. Stabilization of the nanodrug delivery systems by lyophilization using universal step-wise freeze drying cycle. Indian Patent Application No 2559/DEL/2011 filed on September 06, 2011.
39. Swarnakar NK, Thanki K, Jain S. Effect of co-administration of CoQ10-loaded nanoparticles on the efficacy and cardiotoxicity of doxorubicin-loaded nanoparticles. RSC Adv. 2013;3:14671–85.
40. Jain AK, Swarnakar NK, Das M, Godugu C, Singh RP, Rao PR, *et al*. Augmented anticancer efficacy of doxorubicin loaded polymeric nanoparticles after oral administration in breast cancer induced animal model. Mol Pharm. 2011;8(4):1140–51.
41. Chung SY, Sung MK, Kim NH, Jang JO, Go EJ, Lee HJ. Inhibition of P-glycoprotein by natural products in human breast cancer cells. Arch Pharm Res. 2005;28(7):823–8.
42. Shin SC, Choi JS, Li X. Enhanced bioavailability of tamoxifen after oral administration of tamoxifen with quercetin in rats. Int J Pharm. 2006;313(1):144–9.
43. Bachynsky MO, Shah NH, Patel CI, Malick AW. Factors affecting the efficiency of a self-emulsifying oral delivery system. Drug Dev Ind Pharm. 1997;23(8):809–16.
44. Oliver G, Alitalo K. The lymphatic vasculature: recent progress and paradigms. Annu Rev Cell Dev Biol. 2005;21:457–83.
45. Nilsson UW, Dabrosin C. Estradiol and tamoxifen regulate endostatin generation via matrix metalloproteinase activity in breast cancer in vivo. Cancer Res. 2006;66(9):4789–94.
46. Tan W-F, Lin L-P, Li M-H, Zhang Y-X, Tong Y-G, Xiao D, *et al*. Quercetin, a dietary-derived flavonoid, possesses antiangiogenic potential. Eur J Pharmacol. 2003;459(2):255–62.